UC Santa Cruz
UC Santa Cruz Previously Published Works

Title
Color Barcode Decoding in the Presence of Specular Reflection

Permalink
https://escholarship.org/uc/item/8dh4r6b9

Authors
Bagherinia, Homayoun
Manduchi, Roberto

Publication Date
2014-09-12

Peer reviewed

Color Barcode Decoding
in the Presence of Specular Reflection

Homayoun Bagherinia and Roberto Manduchi

University of California, Santa Cruz

Abstract. Color barcodes enable higher information density with respect to traditional black and white barcodes. Existing technologies use small color palettes and display the colors in the palette in the barcode itself for easy and robust decoding. This solution comes at the cost of reduced information density due to the fact that the displayed reference colors cannot be used to encode information. We introduce a new approach to color barcode decoding that uses a relatively large palettes (up to 24 colors) and a small number of reference colors (2 to 6) to be displayed in a barcode. Our decoding method specifically accounts for specular reflections using a dichromatic model. The experimental results show that our decoding algorithm achieves higher information rate with a very low probability of decoding error compared to previous approaches that use a color palette for decoding.

1 Introduction

Barcodes can be characterized by their *information rate*, that is, by the number of bits that can be encoded within a certain barcode size. One way to increase a barcode's information rate is through the use of color. By using a palette of N colors, a barcode can convey $\log_2 N$ times more bits than a traditional black and white barcode. The most successful example of color barcode is Microsoft Tag, which is based on HCCB (High Capacity Color Barcode) technology [1]. HCCB uses a grid of colored triangles with 4 colors to encode data. To ensure robust decoding, HCCB barcodes display the four colors in a set of "reference patches" at known positions in the barcode.

Displaying the reference colors in the barcode enables simple decoding strategies. For example, one may compare each color patch to the reference colors, and select the reference color that is closest to the color of the patch. At the same time, displaying all colors in the palette may be counterproductive, in terms of information rate, when large palettes are used [2]. In other words, for large palette size N, the savings produced by a large variety of color palette are offset by the need to display all colors in the palette. Based on this observation, Bagherinia and Manduchi [2] proposed the use of fairly large palettes with a limited number of reference colors displayed in the barcode. Rather than comparing

a color patch to a reference color, they modeled the joint color variation of the patch and of the reference colors under varying illuminant by a low-dimensional linear space. These subspaces (one per each color in the palette) can be learned offline with training images taken under multiple illuminants. When decoding a barcode image, each patch is analyzed individually, together with the reference colors. Decoding the patch color becomes a problem of associating the vector formed by the patch color and the reference colors to the closest subspace.

The linear model of [2] was built under the assumption of Lambertian surface reflectance, and thus is liable to failure when substantial specular reflection is present in the image. Since the barcode material (e.g. printed paper) is hardly Lambertian, a specular component is to be expected when the barcode is viewed from an angle. Our goal in this work was to extend the model of Bagherinia and Manduchi to explicitly account for specular reflection. We use the dichromatic model [3] to describe the appearance of a surface under specular reflection, and show how this can be included in the subspace-based decoding approach of [2], which is augmented based on the observed color of a white patch. The experimental results on images taken under a wide variety of illuminants and viewing angles show a substantial improvement (in terms of reduced decoding error rate) with respect to the original system that assumed Lambertian surface reflectance. In quantitative terms, we show that, by using a palette with $N = 20$ colors and 4 reference colors displayed in the barcode, we are able to encode a 128-bit message using 34 patches overall with 0 decoding errors in our test set. Compared to the 4-color HCCB standard that displays all 4 colors (and thus requires 68 patches to encode the same message), we achieve a reduction of the barcode size by one half.

2   Related Work

A patent by Han et al. [4], who used reference cells to provide standard colors for correct indexing, is possibly the first reported attempt to use color in a 2-D barcode This technology is marketed by Colorzip Media (colorzip.com). Later examples of color barcode technology include the method by Bulan *et al.* [5], who embed data in two different printer colorant channels via halftone-dot orientation modulation, Grillo et al. [6], who used 4 or 16 colors in a regular QR code, and Kato et al. [7] who selected colors that are maximally separated in a plane of the RGB color cube. Pei et al. used four colors in a color barcode technology named "Continuous Color Barcode Symbols" [8]. Blasinski et al. [9] proposed a framework that exploits the spectral diversity between the color channels (C, M, and Y) used in regular color printers, and the (R, G, B) color channels used in color cameras.

Several existing decoding algorithms (including HCCB [1]) include a color clustering step to identify the most representative colors in the barcode. For example, the method of Sali and Lax [10] uses a k-means classifier to assign the (R,G,B) value of a color patch to one reference color. Color clustering, however,

is not guaranteed to work well with large palettes, and therefore the clustering approach is best suited to small palette sizes.

The use of large color palettes and a small number of reference colors was originally proposed by Wang and Manduchi [11], who studied the problem of information embedding via printed color. Bagherinia and Manduchi [12] attempted to decode a color barcode *without* any reference color by modeling the joint variation of the color of groups of color patches under varying illuminant. Later, the same authors [2] used a similar concept but applied to sets formed by a color patch and a set of reference color patches. As mentioned earlier, our work builds upon the algorithm described in [2].

3   Background and Definitions

A color barcode is created from a set $\mathcal{C}_N$ of N colors (*palette*) and a set $\mathcal{C}_r$ of r reference colors. A color barcode of length $K = n + r$ is defined as the arrangement of n color patches, selected from the palette $\mathcal{C}_N$ and used for information encoding, and the r reference colors of $\mathcal{C}_r$, in any spatial configuration. Decoding the bar code means assigning the color of each one of the n information-carrying patches to the index of the corresponding color in the palette $\mathcal{C}_N$. As with standard color barcodes (e.g. HCCB), we assume that the position of the reference colors in the barcode is known. In this work we will follow the approach of Bagherinia and Manduchi [2], who showed that, by carefully modeling the joint color variation as a function of the illuminant, it is possible to use $r < N$ reference colors and still obtain good decoding performance. In fact, we don't even constrain the set of reference colors $\mathcal{C}_r$ to be a subset of the color palette $\mathcal{C}_N$.

Since each color patch carries $\log_2 N$ bits of information, the barcode carries $n \log_2 N$ bits. In order to encode B bits, one needs this many color patches:

$$K = n + r = \lceil B / \log_2 N \rceil + r \qquad (1)$$

Increasing the palette size N and reducing the number r of reference colors decreases the size K of the barcode, resulting in higher *information rate* [2]. For example, Fig. 1 shows the minimum length K of a color barcode that encodes a message of $B = 128$ bits as a function of the size of the color palette N and of the number of reference colors r. (Note that the HCCB standard with $N = r = 4$ would require $K = 68$ color patches for the same 128-bit message.) For a fixed number r of reference colors, the barcode length K decreases monotonically with the size of the color palettes N. In contrast, if the whole palette is represented by the reference colors ($r = N$), the plot of K at $N = 13$ ($K = 48$), after which adding colors to the palette becomes counterproductive.

While the plot in Fig. 1 suggests that large palettes with few reference colors lead to high information rate, it hides the fact that increasing the palette size typically results in larger decoding error rates, which must be offset by adding more reference colors. Let $P_E(N, r)$ is the probability of decoding error (that is, of misclassifying the color of a patch) for a given palette $\mathcal{C}_N$ and a given set of reference colors $\mathcal{C}_r$. Assuming that decoding errors are statistically independent

events, the *decoding error rate*, that is, the probability of decoding error for the barcode (i.e., of decoding at least one color patch incorrectly) is equal to:

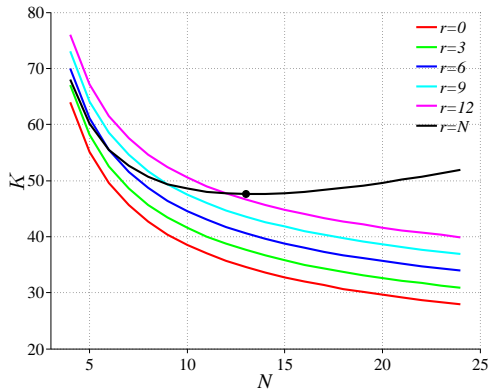$$P_E(N, r, K) = 1 - (1 - P_E(N, r))^{K-r} \qquad (2)$$

Fig. 1. The minimum number of patches K required to encode a 128-bit message versus the size of the palette N.

One may expect $P_E(N, r)$ to increase with increasing N (larger palette) and decrease with increasing r (more reference colors). This was verified experimentally in [2]. This relation establishes a design trade-off between decoding error probability and information rate, mediated by the parameters N and r.

4   Subspace-Based Decoding

4.1   The Lambertian Case

We will follow the general approach of Bagherinia and Manduchi [2] for illumination-invariant color patch decoding, briefly summarized in the following. Consider a patch colored with the i-th color in the palette $\mathcal{C}_N$. The observed color $\mathbf{c}_i = [c_{i,R}, c_{i,G}, c_{i,B}]^T$ of this patch will vary as the illuminant changes (e.g., from sunlight to artificial light), making color identification difficult. The key observation of [2] is that the *joint* color variation of a set of color patches, all under the same illumination, is bound by a linear constrain. For example, consider the $3(r+1)$–dimensional vector $\mathbf{e}_i = [\mathbf{c}_i, \mathbf{d}_1, \dots, \mathbf{d}_r]^T$ which includes the colors of the (known) reference patches $\{\mathbf{d}_j\}$, with $\mathbf{d}_j = [d_{j,R}, d_{j,G}, d_{j,B}]^T$. If the surfaces are Lambertian, and assuming that the illuminant spectra live in a finite-dimensional subspace of dimension N_{ill}, then the vector $\mathbf{e}_i$ must live in a linear subspace $\mathcal{S}_i$

of dimension equal to $\min(3(r+1), N_{\mathrm{ill}})$, which can be considered equal to N_{ill} for $r \geq 1$ [13, 14]. Formally:

$$\mathbf{e}_i = \boldsymbol{\Phi}_i \mathbf{v} \tag{3}$$

where $\mathbf{v}$ is a N_{ill}–vector that represents the illuminant, and $\boldsymbol{\Phi}_i$ is a matrix that characterizes the reflectivity of the patch surface[1]. It is useful to define the *dimensionality ratio (DR)* as the ratio between the dimension of the embedding subspace $\mathcal{S}_i$ and the dimension of $\mathbf{e}_i$:

$$\mathrm{DR} = \frac{N_{\mathrm{ill}}}{3(r+1)} \tag{4}$$

This suggests a simple algorithm for decoding a generic color patch $\mathbf{c}$: (1) Build the vector $\mathbf{e}$ (by juxtaposing the observed color $\mathbf{c}$ with the observed colors of the reference patches in the same barcode); (2) Find the subspace $\mathcal{S}_i$ that is closest to the vector $\mathbf{e}$; (3) Decode $\mathbf{c}$ as i. Intuitively, the smaller the dimensionality ratio DR (itself an decreasing function of r), the higher the robustness of this decoding algorithm with respect to noise. This formalizes the intuitive notion that more reference colors should ensure lower decoding error rates.

The subspaces $\mathcal{S}_i$ for $1 \leq i \leq N$ can be learnt from observation of the colors in $\mathcal{C}_N \cup \mathcal{C}_r$ under a wide variety of illuminants. If multiple pictures of the color patches under different illuminants are impractical or impossible to obtain, one may "constrain" the embedding subspaces $\mathcal{S}_i$ by means of the diagonal (von Kries) model of color change. Indeed, under the diagonal color model, the matrix $\boldsymbol{\Phi}_i$ can be written as [2]

$$\boldsymbol{\Phi}_i^T = \begin{bmatrix} c_{i,R} & 0 & 0 & d_{1,R} & 0 & 0 & d_{2,R} & \cdots \\ 0 & c_{i,G} & 0 & 0 & d_{1,G} & 0 & 0 & \cdots \\ 0 & 0 & c_{i,B} & 0 & 0 & d_{1,B} & 0 & \cdots \end{bmatrix} \tag{5}$$

It is easy to see that this matrix can be learnt from observation of the colors under just one illumination. However, the resulting deciding error rate are typically higher than with the "unconstrained" subspace approach [2].

4.2   The General Case

In the real world, surfaces are rarely Lambertian, and the reflected light should be expected to contain a specular component. The amount of this specular component depends on the surface characteristics and on the joint illumination/viewing geometry. For color barcodes printed on paper, the specular component can be quite noticeable [2, 15].

A simple model of light reflection that accounts for specular reflection is the *dichromatic model* [3]:

$$\mathbf{c} = m^{(b)} \mathbf{c}^{(b)} + m^{(i)} \mathbf{c}^{(i)} \tag{6}$$

---

[1] Note that $\boldsymbol{\Phi}_i$ is also a function of the spectral sensitivities of the color filters at the camera.

The dichromatic model states that the observed color $\mathbf{c}$ of a surface is the sum of two colors, $\mathbf{c}^{(b)}$ (*body reflection*) and $\mathbf{c}^{(i)}$ (*interface reflection*), weighted by coefficients $m^{(b)}$ and $m^{(i)}$ that can take values between 0 and 1. It is normally assumed that $m^{(b)}$ (the "Lambertian component") is largely independent of changes in the viewpoint (and thus can be safely set it to 1). For most materials, the interface reflection $\mathbf{c}^{(i)}$ can be considered material-independent and equal to the color of the illuminant itself (or, equivalently, of a white surface reflecting the same illuminant). In practice, the dichromatic model predicts that the specular (interface) reflection "steers" the color of the surface towards the color of a white surface seen under the same illuminant. This observation suggests that if the barcode contains a white reference patch, the color of this white patch may be used to "remove" the specular component from the color of other patches, provided that one can somehow estimate the coefficient $m^{(i)}$ at each patch.

Formally, we can model the color of the vector $\mathbf{e}$ defined in the previous section as follows:

$$\mathbf{e}_i = \boldsymbol{\Phi}_i \mathbf{v} + \mathbf{W}\mathbf{m}^{(i)} \tag{7}$$

with

$$\mathbf{W} = \mathbf{I} \otimes \mathbf{w} = \begin{bmatrix} \mathbf{w} & \mathbf{0} & \mathbf{0} & \cdots \\ \mathbf{0} & \mathbf{w} & \mathbf{0} & \cdots \\ \vdots & \vdots & \vdots & \ddots \end{bmatrix} \tag{8}$$

where $\mathbf{I}$ is the $(r+1) \times (r+1)$ identity matrix, $\otimes$ represents the Kronecker product, $\mathbf{w}$ is the observed color of the white reference patch, and $\mathbf{m}^{(i)}$ is a $(r+1)$–vector containing the interface reflection coefficients for all patches in $\mathbf{e}$. This suggests that the subspace approach used for the Lambertian case could be extended to the general case with specularities, owing to the observed white patch. However, it should be noticed that the the presence of specular reflection increases the dimensionality[2] of the embedding space $\mathcal{S}$ to $N_{\text{ill}} + r$. With respect to the Lambertian case, the dimensionality ratio DR is thus increased by a factor of $1 + r/N_{\text{ill}}$, making decoding harder.

In order to keep the dimensionality ratio under control, in this work we assume that $m^{(i)}$ is constant across patches for a fixed illuminant. This simplifying assumption can be partly justified by the fact that, for a small sized planar barcode, the viewing geometry can be considered approximately constant for all patches. Hence, assuming constant $m^{(i)}$ across patches means neglecting the difference between interface reflection coefficients for the different patches in the barcode. This approximation allows us to rewrite Eq. (7) as follows:

$$\mathbf{e}_i = \begin{bmatrix} \boldsymbol{\Phi}_i & | & \mathbf{V} \end{bmatrix} \begin{bmatrix} \mathbf{v} \\ m^{(i)} \end{bmatrix} \tag{9}$$

---

[2] Note that the white patch is assumed to be part of the reference colors. For this patch, the specular reflection component is immaterial. This is the reason why the dimension of the embedding space is $N_{\text{ill}} + r$ rather than $N_{\text{ill}} + r + 1$.

with $\mathbf{V} = [\mathbf{w}^T, \dots, \mathbf{w}^T]^T$ obtained from the observed color of the white reference patch. With this simplification, the dimensionality ratio DR is only increased by a factor of $1 + 1/N_{\text{ill}}$ with respect to the Lambertian case.

Note that the matrix $\boldsymbol{\Phi}_i$ is computed from training data in the absence of specular reflection. In practice, this can be achieved by ensuring that, when taking training images, the color patches lie on a plane orthogonal to the camera's optical axis. Also note that, in order to compute the distance of the vector $\mathbf{e}$ to a subspace $\mathcal{S}_i$, it is useful to first derive an orthogonal column basis for $[\boldsymbol{\Phi}_i|\mathbf{V}]$, which can be achieved via QR decomposition.

5 Experimental Evaluation

We ran a number of experiments with color checkerboards printed on paper with a regular color printer. Images were taken of the checkerboards with a Canon EOS 350D camera in raw (CR2) format with a resolution of 3474x2314 pixels and 12 bits per color channel.

5.1 Training Set and Model Construction

In order to select the palette and the reference colors, we started with a "training" checkerboard with 125 colors, uniformly sampled in (R,G,B) color space. We took multiple images of this checkerboard from a constant distance of about 1.5 meters, with the camera's optical axis orthogonal to the checkerboard to minimize specular reflections, under 32 different illumination conditions. The color values within each patch were averaged together to reduce noise.

We used the method described in [2], and briefly summarized in the following, to select the color palettes $\mathcal{C}_{12} \subset \mathcal{C}_{16} \subset \mathcal{C}_{20} \subset \mathcal{C}_{24}$, together with 5 reference colors. For each illuminant, we clustered the colors of the patches using k-means with 24 clusters. We then selected the 24 cluster centers with highest occurrences among all illuminants. We repeated the same procedure to select the colors of the palettes for $N = 20, 16$ and 12, each time starting from the palette chosen in the previous step.

The reference colors were sampled from the 125-24=101 colors that were not used for the color palette $\mathcal{C}_{24}$. (Note that choosing reference colors from the palette would actually *increase* the dimensionality ratio DR from $N_{\text{ill}}/3(r+1)$ to $N_{\text{ill}}/3r$, making decoding harder.) We used a greedy recursive strategy for jointly selecting r reference colors (with $1 \leq r \leq 5$) and the dimensionality of the embedding subspaces $\{\mathcal{S}_i\}$, which was kept constant across subspaces for given r. Reference patches are added one at a time. Given the current set of r reference colors, all possible remaining $125 - 24 - r$ colors and subspace dimensions from 1 to 5 are tested using cross-validation over multiple illuminants, and the marginal error rates $P_E(N, r)$ are computed. The reference color and subspace dimension that minimize the decoding error rate are selected and added to the set. For $r = 1, 2$ the algorithm chose an embedding subspace dimension 3, while for $r = 3, 4, 5$ the chosen subspace dimension was of 4. The white patch
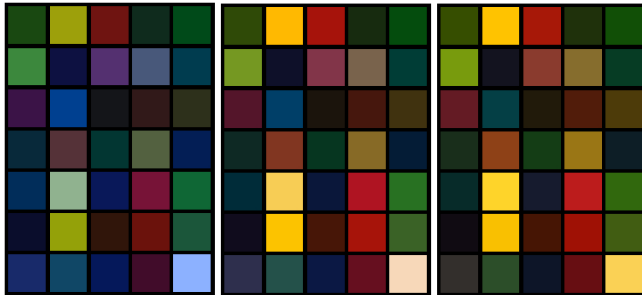
Fig. 2. A collage created with the chosen palette colors and reference colors, seen under three different illuminant spectra. The patches are distributed in such a way that, in lexicographic order, the first N patches form $\mathcal{C}_N$ for $N = 12, 16, 20, 24$. Following are the 5 reference colors chosen for the "unconstrained" subspace decoding algorithm, followed by the 5 reference patches chosen using the diagonal color model. The last patch is the white patch.

was then added to the reference colors when the dichromatic model was used. Note that the decoding error was computed under the assumption of Lambertian surfaces (3). Also note that we generated two sets of reference patches, one for the "unconstrained" embedding subspace model, and one for the diagonal model (5).

Along with the palette and the reference colors, we computed the embedding subspaces (represented by the matrices $\{\boldsymbol{\Phi}_i\}$ in (3)) for all combinations of palette size N and number of reference patches r, using data from all 32 illumination conditions. Additionally, we learnt the matrices $\{\boldsymbol{\Phi}_i\}$ using the diagonal model (5) for all combinations (N, r). However, since these matrices can be learnt from just one image, we created 32 versions of each $\boldsymbol{\Phi}_i$, one per illumination condition.

The color palettes and reference colors chosen with this algorithm are shown in Fig. 2.

5.2   Test Set and Results

We evaluated the performance of our proposed decoding algorithms using a 13×12 "test" color checkerboard with size of 16.5×15 cm, printed with the same color printer used for the "training" checkerboard. The first six pairs of rows each contain all 24 colors in the palette, in random order. The last row contains the five reference colors selected for the unconstrained subspace model, followed by the five reference colors chosen for the diagonal model and by two white patches. In order to facilitate automatic checkerboard detection and patch localization in our pictures, we printed a thick black edge outside the pattern, outlining a visible white frame (see Fig. 3). (This design was inspired by the ARToolKit marker concept [16].) Of course, in a real application, a smaller frame (or no frame at all) would have to be used.

Fig. 3. Examples of images with the "test" color checkerboard, used in our experimental tests. The inset at each picture shows the brightness-rescaled, zoomed-in checkerboard detail.

We took 100 images from the test checkerboard under multiple illumination conditions, multiple viewing angles (ranging from -45 to 45 degrees with respect to the normal to the checkerboard surface), and multiple distances (1 to 5 meters). Figure 3 shows some examples of our test images. Each color patch was automatically localized, and color values within the central area of the patch were averaged together to reduce noise (resulting in one color value per patch).

We evaluated the marginal error rate $P_E(N, r)$ for a combination of design choices: (a) using the unconstrained vs. the diagonal subspace model (5); (b) using the Lambertian reflection model (3) vs. the dichromatic reflection model (9). For each design choice, we considered all combinations of parameters[3] N and r. For each pair (N, r) we used the associated matrices $\{\Phi_i\}$ learnt from the "training" checkerboard as discussed above.

When using the unconstrained subspace model, the error rate $P_E(N, r)$ was given by the total number of color patches in the "test" checkerboard that were incorrectly decoded, divided by the number of images (100) and by the number of color patches in the colorchecker ($N \times 6$). The computation of the error rate using the diagonal model (5) is slightly different, as in this case there are 32 different versions of each matrix Φ_i, one per illumination condition. We tested all such matrices, and computed the error rate as the total number of color patches in the "test" checkerboard that were incorrectly decoded, divided by the number of images (100), by the number of color patches in the colorchecker ($N \times 6$), and by the number of illumination conditions in the training dataset (32).

---

[3] Note that, when using the dichromatic model, we added the white patch to the sets of reference colors used for the Lambertian reflection model, resulting in a number of reference patches larger by one.
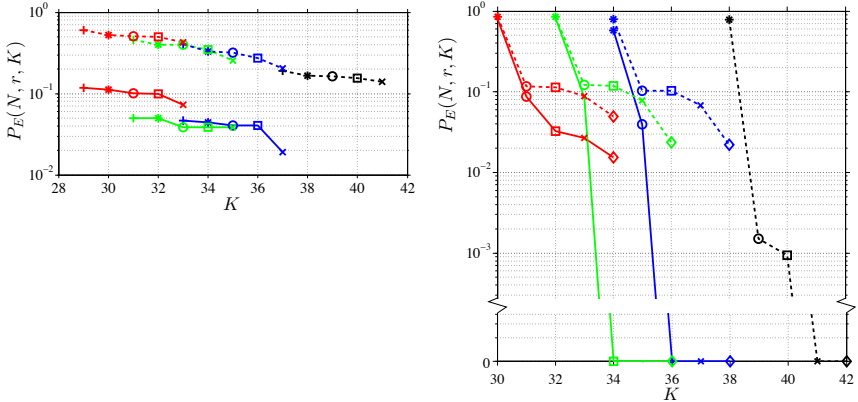
Fig. 4. The probability $P_E(N, r, K)$ of decoding error for a 128-bit message as a function of the total barcode length K, the palette size N, the number of reference colors r, and the embedding subspace type. Black: $N = 12$; Blue: $N = 16$; Green: $N = 20$; Red: $N = 24$. '+': $r = 1$; '*': $r = 2$; 'o': $r = 3$; '□': $r = 4$; '×': $r = 5$; '◇': $r = 6$. Solid line: unconstrained embedding subspace; Dotted line: diagonal model (5). Left: Assuming Lambertian reflectance (3), with r ranging from 1 to 5. Right: Using the dichromatic reflection model (9), with r ranging from 2 to 6 (the white patch was added to the chosen set of reference colors.)

The resulting error rates $P_E(N, r, K)$ for a message with $B = 128$ bits are shown in Fig. 4. As expected, the error rate decreases with increasing barcode length K. The diagonal model is also shown to perform poorly compared to the unconstrained model (as also found in [2]). Using the dichromatic model results in improved performance for large enough r. Indeed, for $N = 20$ and $r = 4$, we achieve 0 error rate for $K = 34$ in our data set. This is a very promising result, considering that the same parameters yield an error rate of 0.07 using the Lambertian reflection model. To put this result in context, consider that, as discussed in Sec. 3, a system that represents all the palette colors in the reference set ($N = r$) requires a barcode of length K equal to at least 48 (for $N = 13$) to encode 128 bits. By using a smaller number of color patches and the dichromatic model, our algorithm is able to pack the same amount of information in a barcode that is 30% smaller. With respect to the HCCB system with $N = r = 4$ (which requires $K = 68$ patches for a 128-bit message), our algorithm allows for reduction of the barcode size by half.

When using the diagonal model, an error rate of less than 0.001 is obtained only for $K \geq 40$. In this case, there is a smaller (but still significant) gain in terms of information rate with respect to the case $N = r$. As discussed earlier, the practical advantage of the diagonal model is that it requires only one picture of the color palette, rather than multiple pictures under a variety of illumination condition as needed by the unconstrained subspace model.

6   Conclusions

We have introduced a new algorithm for color barcode decoding in presence of specular reflection. Our experiments have shown that, by selecting up to 24 colors and a small number of reference colors, it is possible to achieve higher information rate than with mainstream color barcode decoding methods while ensuring low decoding error rates. Future research will consider other sources of error such as due to blur-induced color mixing from two nearby patches or to color barcodes printed from different printers.

7   Acknowledgement

References

1. D. Parikh and G. Jancke, "Localization and segmentation of a 2D high capacity color barcode," in *Applications of Computer Vision, 2008. WACV 2008. IEEE Workshop on.* IEEE, 2008, pp. 1–6.
2. H. Bagherinia and R. Manduchi, "High information rate and efficient color barcode decoding," in *International Workshop on Color and Photometry in Computer Vision (CPVC).* Springer, 2012, pp. 482–491.
3. S. A. Shafer, "Using color to separate reflection components," *Color Research & Application*, vol. 10, no. 4, pp. 210–218, 1985.
4. T. Han, C. Cheong, N. Lee, and E. Shin, "Machine readable code image and method of encoding and decoding the same," U.S. Patent 7020327, 2000.
5. O. Bulan, V. Monga, and G. Sharma, "High capacity color barcodes using dot orientation and color separability," in *Proc. SPIE-IS&T Electronic Imaging*, 2009, vol. 7254.
6. A. Grillo, A. Lentini, M. Querini, and G.F. Italiano, "High capacity colored two dimensional codes," in *Proc. Int. Multiconf. on Comp. Science Inf. Tech.*, 2010.
7. H. Kato, K.T. Tan, and D. Chai, "Novel colour selection scheme for 2D barcode," in *Proc. International Symposium on Intelligent Signal Processing and Communication Systems (ISPACS 2009)*, 2009.
8. S. Pei, G. Li, and B. Wu, "Codec system design for continuous color barcode symbols," in *Proceedings of the 2008 IEEE 8th International Conference on Computer and Information Technology Workshops*, Washington, DC, USA, 2008, pp. 539–544, IEEE Computer Society.
9. H. Blasinski, O. Bulan, and G. Sharma, "Per-colorant-channel color barcodes for mobile applications: An interference cancellation framework," *IEEE Transactions on Image Processing*, vol. 22, no. 4, pp. 1498–1511, 2013.
10. E. Sali and D. Lax, "Color bar code system," 2006, U.S. Patent 7210631.
11. F. Wang and R. Manduchi, "Color-constant information embedding," in *Proc. IEEE Workshop on Color and Reflectance in Imaging and Computer Vision*, 2010.
12. H. Bagherinia and R. Manduchi, "A theory of color barcodes," in *IEEE Color and Photometry in Computer Vision Workshop (CPVC 2011)*. IEEE, 2011, pp. 806–813.

13. D.B. Judd, D.L. MacAdam, G. Wyszecki, H.W. Budde, H.R. Condit, S.T. Henderson, and J.L. Simonds, "Spectral distribution of typical daylight as a function of correlated color temperature," *JOSA*, vol. 54, no. 8, pp. 1031–1040, 1964.
14. D. Slater and G. Healey, "What is the spectral dimensionality of illumination functions in outdoor scenes?," in *Proc. CVPR*. IEEE, 1998.
15. H. Bagherinia and R. Manduchi, "Robust real-time detection of multi-color markers on a cell phone," *Journal of real-time image processing*, vol. 8, no. 2, pp. 207–223, 2013.
16. H. Kato, M. Billinghurst, B. Blanding, and R. May, "Artoolkit," Tech. Rep., Hiroshima City University, 1999.